JOURNAL OF GEOPHYSICAL RESEARCH, VOL. 95, NO. A4, PAGES 3745-3754, APRIL 1, 1990

Periodic Features in the Alfvén Wave Wake of Io

ANDREW N. WRIGHT

Astronomy Unit, School of Mathematical Sciences, Queen Mary and Westfield College, London, England

PETER R. SMITH

Electronic and Electrical Engineering Department, University of Loughborough, Leicestershire, England

The evolution of Io's Alfvén waves is modeled in a realistic magnetic field and torus density distribution. This is performed by calculating the normal modes of the field lines disturbed by Io and synthesising the waves near Io from a complex sum over the eigenmodes. The wave pattern produced downstream from the satellite exhibits periodic structure over a range of scales. In terms of the Jovian longitude (or CML) of a stationary observer, we expect large-scale structure ($> 60°$), small-scale structure ($< 6°$), and intermediate periods too. These are close to observed intervals in decametric (DAM) emissions, such as the length of a DAM storm, bunching of arcs within a storm, and individual arc separation.

1. INTRODUCTION

Io is one of the four large Jovian satellites discovered by Galileo in 1610. However, it was not until the second half of the present century that we began to realize that Io is one of the most exotic moons in our solar system. *Bigg* [1964] reported that the decameter emissions from Jupiter were strongly influenced by the position of Io. Shortly afterward, *Goldreich and Lynden-Bell* [1969] proposed that the satellite was a good electrical conductor and would set up an unusual current system as it moved relative to the Jovian magnetoplasma. Observations of optical sodium emissions from Io and its vicinity [*Brown*, 1974] suggested that matter was picked-up from Io by the Jovian magnetosphere. Other emission lines reveal the presence of potassium, sulphur, and oxygen. The Voyager missions to Jupiter permitted a detailed examination of the Jovian system. They confirmed that material was escaping from Io, sometimes via volcanic eruptions. Matter lost from Io tends to remain in the vicinity of the satellite's orbit initially, and produces a density enhancement in that region. This is known as the Io plasma torus [*Bridge et al.*, 1979; *Broadfoot et al.*, 1979]. The increased plasma density near Io (and the associated reduction in Alfvén speed) means that the current system proposed by *Goldreich and Lynden-Bell* [1969] requires modification. The current flowing within the satellite will close in Alfvén waves that are launched downstream, along the Alfvénic characteristics [*Drell et al.*, 1965]. Several authors have modeled the disturbance near Io in this fashion [*Goertz and Deift*, 1973; *Herbert*, 1985; *Barnett and Olbert*, 1986; *Neubauer*, 1980; *Southwood et al.*, 1980; *Wolf-Gladrow et al.*, 1987; *Wright and Southwood*, 1987; *Linker et al.*, 1988]. Voyager 1 flew very close to the Alfvén wings near Io and measured the disturbance. The magnetic field perturbation [*Acuña et al.*, 1981], and the plasma bulk velocity perturbation [*Belcher et al.*, 1981; *Barnett*, 1986] are in excellent agreement with the Alfvén wave model. The disturbance to energetic particles [*Lanzerotti et al.*, 1981] is also consistent with the presence of Alfvén waves [*Schulz and Eviatar*, 1977; *Goldstein and Ip*, 1983; *Wright*, 1987*a*].

The Planetary Radio Astronomy instruments aboard Voyagers 1 and 2 revealed new detail in the DAM emissions [*Warwick et al.*, 1979*a*,*b*]. An example is shown in Figure 1. The most striking feature of the frequency-time DAM spectrographs is the nested arc-like structures. The first panel in Figure 1 contains vertex-early arcs, while the second panel has vertex-late arcs. Warwick et al. noted that an individual arc could be produced by allowing decameter emission at the local electron gyrofrequency to be beamed along the surface of a cone whose axis is aligned with the local magnetic field direction. As the field line rotates relative to the observer, an arc is produced in the spectrograph. Whether the arc is vertex-early or vertex-late depends upon whether the field line is rotating towards or away from the observer. It is thought that the current extending away from Io (in the Alfvén wings) is a likely source of energy for the decameter radiation. The electron cyclotrotron maser instability could be the mechanism which excites these DAM emissions [*Goldstein and Goertz*, 1983]. The origin of the multiple arcs was addressed by *Gurnett and Goertz* [1981]. They considered the long-term evolution of the waves launched from Io by using WKB theory. In this limit, the Alfvén waves propagate along the magnetic field lines to the Jovian ionosphere. There is complete transmission of the wave through the inhomogeneous magnetoplasma and efficient reflection at the ionospheric boundary. The waves bounce between the ionospheres and drift downstream from the satellite, thus establishing a stationary periodic wake (in the rest frame of Io). Gurnett and Goertz suggested that each Alfvén wave bounce would produce a DAM arc, and so it was possible to understand the multiple arcs found in the data. *Bagenal* [1983] continued this approach and performed ray-tracing calculations of the wave trajectories. Recently, *Staelin et al.* [1988] have compared the observed arc spacing and the WKB, or ray-tracing, arc spacing. They found that the observed spacing was typically 2.7 times less than the predicted one. For

Paper number 89JA02768.
0148-0227/90/89JA-02768$05.00

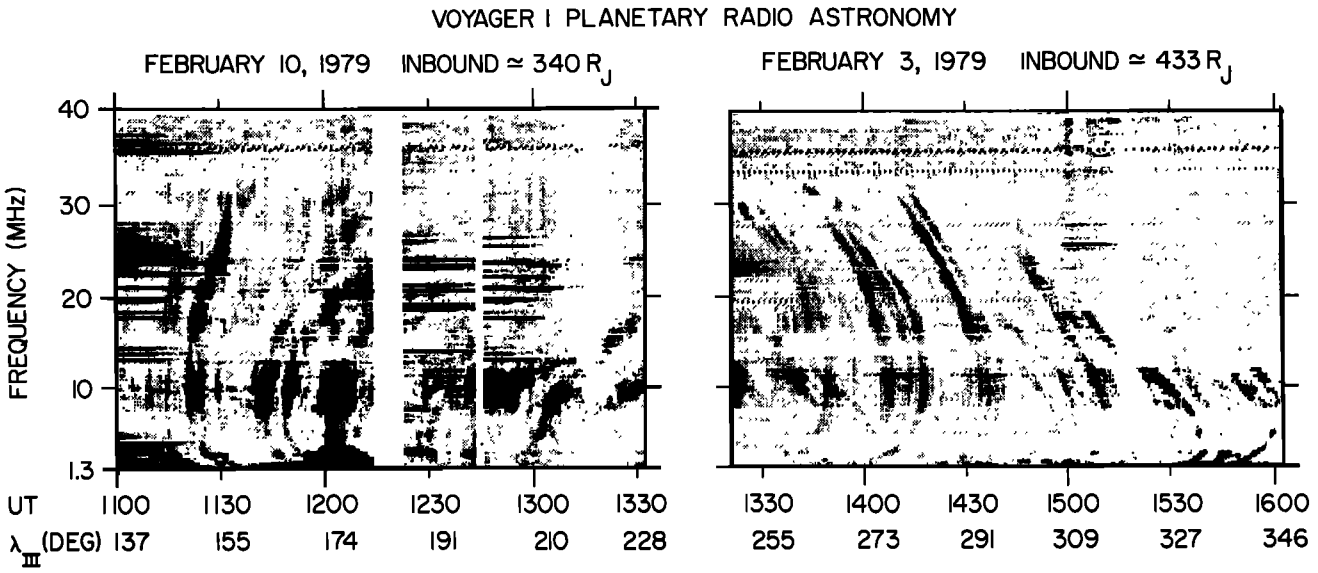

Fig. 1. DAM spectra (emission frequency against time). Note the range of important scales in the spectra e.g., the separation of arcs and the bunching of individual arcs together.

example, a round trip travel time for a single Alfvén wave of 24 min would produce a periodicity of 24° in spacecraft Central Meridian Longitude (s/c CML) in Figure 1. *Bagenal and Leblanc* [1988] have tried to resolve this discrepancy by suggesting that each Alfvén wave bounce triggers a set of DAM arcs, rather than an individual arc. However, it is not understood how several arcs can be produced by one wave bounce.

Neubauer [1980] commented that the enormous increase in Alfvén speed along Io's L shell could produce significant wave reflection, particularly at the torus boundary. Detailed studies of the wave propagation over the past few years [*Wright*, 1987*b*; *Wright and Schwartz*, 1989] suggest that over half of the Alfvén wave power launched from Io will be reflected by the change in propagation speed. This implies that the WKB limit is invalid and ray-tracing notions are inappropriate. To investigate the problem further, we have considered the waves in terms of the normal modes of field lines in Io's L shell. Preliminary results from this type of model [*Smith and Wright*, 1989] reveal periodic structure on a range of scales similar to those found in data. In this paper we present a detailed description of the eigenmode model and comprehrensive results from simulations.

The paper is structured in the following fashion; section 2 develops the model; section 3 presents the results; section 4 interprets the periodicities found in section 3; section 5 reviews the periods found in DAM observations and compares them with periods found in the model; and finally, section 6 summarizes the paper.

2. The Model

The model used throughout this paper is based upon decoupled toroidal and poloidal field line motions in a cold plasma. It is well-known that the motions decouple in a variety of highly symmetric and asymmetric situations [*Dungey*, 1967; *Radoski*, 1967], or in the absence of a compressional field perturbation [*Singer et al.*, 1981]. (See the appendix.) Voyager 1 and Pioneer 10 data do indeed confirm that the compressional perturbation is small [*Walker and Kivelson*, 1981; *Acuña et al.*, 1981], both near and far from Io. Thus we feel justified in using decoupled modes in this paper.

The coordinate system used throughout is an orthogonal curvilinear one, whose γ axis lies parallel to the local magnetic field direction [see, e.g., *Singer et al.*, 1981; *Wright*, 1987*b*]. Since we shall employ a dipolar background magnetic field, one of the other coordinates (say β) may be proportional to the azimuth about the axis of symmetry. The final coordinate (α) would then label the L shells. In a dipolar magnetic field the radial vector is related to the latitude by $r = r_o \cos^2\lambda$. Hence the scale factor h_β (see appendix) will be proportional to $r_o \cos^3\lambda$. The choice of the scale factor h_α has a degree of arbitraryness. We shall take it to be proportional to $r_o^2 \cos^3\lambda/\sqrt{1+3\sin^2\lambda}$, since this means that the function (defined in the appendix) $f(\alpha,\beta) = \text{const}$. By combining the momentum and induction equations given in the appendix and noting that the spatial derivative along a field line $(1/h_\gamma).(\partial/\partial\gamma)$ is equal to $\left[r_o \cos\lambda.\sqrt{1+3\sin^2\lambda}\right]^{-1} d/d\lambda$, we find

$$\frac{d}{d\lambda}\left(\frac{1+3\sin^2\lambda}{L_I\rho_n\cos^{13}\lambda}\cdot\frac{db_\alpha^*}{d\lambda}\right)+\omega^2 L_I\cos\lambda\left[1+3\sin^2\lambda\right]b_\alpha^*=0 \tag{1}$$

$$\frac{d}{d\lambda}\left(\frac{1}{L_I\rho_n\cos^{13}\lambda}\cdot\frac{db_\beta^*}{d\lambda}\right)+\omega^2 L_I\cos\lambda b_\beta^*=0$$

where $b_\alpha^* = b_\alpha\cos^3\lambda/\sqrt{1+3\sin^2\lambda}$ and $b_\beta^* = b_\beta\cos^3\lambda$. The density profile ($\rho_n$) is similar to that used in other studies [*Wright*, 1987*b*], and is modeled as a Gaussian distribution (of half-width one Jovian radius) that falls off to a constant background value. L_I is the L shell of Io's orbit and is taken to be 5.9. The velocity perturbations are governed by the following equations:

$$\frac{d}{d\lambda}\left(\frac{1}{L_I\cos\lambda[1+3\sin^2\lambda]}\cdot\frac{du_\alpha^*}{d\lambda}\right)+\omega^2 L_I\frac{\rho_n\cos^{13}\lambda}{1+3\sin^2\lambda}u_\alpha^*=0 \tag{2}$$

$$\frac{d}{d\lambda}\left(\frac{1}{L_I\cos\lambda}\cdot\frac{du_\beta^*}{d\lambda}\right)+\omega^2 L_I\rho_n\cos^{13}\lambda u_\beta^*=0$$

$u_\alpha^* = u_\alpha\sqrt{1+3\sin^2\lambda}/\cos^3\lambda$ and $u_\beta^* = u_\beta/\cos^3\lambda$. All of the perturbations $(b_m, u_m; m = \alpha, \beta)$ form Sturm-Liouville systems; however, the systems for (b_m^*, u_m^*) are more convenient to integrate. We shall solve equations (1) and (2), from which the velocity and magnetic field eigenmodes are easily found using the relations above. In order to solve for the eigenmodes, we need to specify the boundary conditions. Since both ends of the field lines are embedded in the ionosphere, the velocity perturbation will be required to vanish there. The numerical solutions were derived using the 'shooting method' in conjunction with a fourth-order Runge-Kutta scheme [see, e.g., *Carnaham et al.*, 1969].

The eigenfunctions of a Sturm-Liouville system are orthogonal to one another when weighted with the weighting function (P) for that system,

$$\int_{-\lambda_o}^{\lambda_o} F_{mi} F_{mj} P d\lambda = \delta_{ij} \tag{3}$$

The invariant latitude for Io's L shell is taken as $\lambda_o = 65°$. F_{mi} and F_{mj} represent the ith and jth modes of either u or b. P is equal to $L_I\cos^7\lambda$ for both field components and $\rho_n L_I\cos^7\lambda$ for both velocity components.

It is a useful property of Sturm-Liouville systems that we are able to synthesize an arbitrary disturbance on the field line as a complex sum of the appropriate modes. To do this, at $t = 0$, all we need know is $\mathrm{b}(\lambda, t = 0)$ and $\partial\mathrm{b}(\lambda, t = 0)/\partial t$. For example, perturbations on the field line (α_0, β_0) in Io's L shell may be written as the real part of the following sum:

$$b_m(\lambda, t) = \sum_{j=1}^{\infty} C_{mj} b_{mj}(\lambda)\cdot e^{i[\omega_{mj}t+\phi_{mj}]} \tag{4}$$

In this notation, $b_{mj}(\lambda)$ is the shape of the jth eigenmode, and ω_{mj} is its eigenfrequency. The (real) coefficient C_{mj} and the phase ϕ_{mj} are determined from the conditions at $t = 0$. The rate of change of the magnetic field perturbation can be found by differentiating equation (4), and again taking the real part,

$$\frac{\partial b_m}{\partial t} = \sum_{j=1}^{\infty} i\omega_{mj} C_{mj} b_{mj}(\lambda)\cdot e^{i[\omega_{mj}t+\phi_{mj}]} \tag{5}$$

The coefficients and phases can be found from the real parts of the following series of integrals:

$$\begin{aligned} I_{mj} &= \int_{-\lambda_o}^{\lambda_o} P b_m b_{mj} d\lambda \\ J_{mj} &= \int_{-\lambda_o}^{\lambda_o} P\cdot\frac{\partial b_m}{\partial t}\cdot b_{mj} d\lambda \end{aligned} \tag{6}$$

C_{mj} and ϕ_{mj} are then given by

$$\begin{aligned} C_{mj}^2 &= I_{mj}^2 + \frac{J_{mj}^2}{\omega_{mj}^2} \\ \tan(\phi_{mj}) &= \frac{-J_{mj}}{\omega_{mj} I_{mj}} \end{aligned} \tag{7}$$

Since the waves leaving Io will propagate according to the WKB limit in Io's immediate vicinity [*Goertz*, 1980; *Wright*, 1987*b*; *Wright and Schwartz*, 1989], it is possible to write down explicit expressions for the perturbed fields just behind the satellite [*Neubauer*, 1980; *Wright and Southwood*, 1987]. By synthesizing this perturbation it will be possible to calculate the temporal evolution of a field line by evaluating equation (4) at later times. Since the field lines also drift away from the satellite with time, this will also yield the structure of the stationary wave disturbance viewed from Io's rest frame.

3. PERTURBED FIELD LINE EVOLUTION

Throughout this paper we shall make use of dimensionless units, unless stated otherwise. These units are based upon the Jovian radius ($1\ R_J = 7.14\times10^4\ km$) and an equatorial Alfvén speed of 250 $km\ s^{-1}$. Thus our basic time unit is 4.76 min. The ray-tracing period for a pair of Alfvén waves is 2.5291 and is associated with the WKB bounce angular frequency $\omega_B = 2.4843$. If ray-tracing notions are valid the expected eigenfrquencies of both the toroidal and poloidal modes would be $\omega_{mj} = \frac{1}{2}(j+1)\omega_B$, where $j = 0$ corresponds to the fundamental mode. The toridal modes have already been discussed [*Smith and Wright*, 1989] so we shall concentrate on the poloidal modes from here on and drop the subscript m.

The eigenfrequencies of the poloidal modes are given in the second column of Table 1. The poloidal frequencies differ greatly from the WKB estimate for the first few modes but are in much better agreement for the higher frequencies. This is due to the ray-tracing approximation becoming less invalid at higher ω. For example, the third harmonic differs from the WKB estimate by 10%, while the twentieth is only out by 1%. The poloidal eigenfrequencies are generally much closer to the corresponding toroidal frequency (see the values given by *Smith and Wright*, [1989]). The poloidal frequencies are always slightly less than the toroidal ones but agree with one another to better than 1% for the second

TABLE 1. The Frequencies and Associated Intervals of the Poloidal Modes

Harmonic	ω	τ_p	$\Delta\phi_I$	τ_o	ΔCML_o
Fund.	0.3694	80.966	37.576	265.74	160.77
1st	1.8766	16.030	7.439	52.61	31.83
2nd	3.191	9.373	4.350	30.76	18.61
3rd	4.484	6.670	3.096	21.89	13.25
4th	5.764	5.189	2.408	17.03	10.30
5th	7.035	4.251	1.973	13.95	8.84
6th	8.302	3.603	1.672	11.82	7.15
7th	9.565	3.127	1.451	10.26	6.21
8th	10.825	2.763	1.282	9.07	5.49
9th	12.082	2.475	1.149	8.13	4.92
10th	13.338	2.242	1.041	7.36	4.45
11th	14.592	2.050	0.951	6.73	4.07
12th	15.845	1.888	0.876	6.20	3.75
13th	17.097	1.749	0.812	5.74	3.47
14th	18.348	1.630	0.757	5.35	3.24
15th	19.598	1.526	0.708	5.01	3.03
16th	20.846	1.435	0.666	4.71	2.85
17th	22.095	1.354	0.628	4.44	2.69
18th	23.342	1.281	0.595	4.21	2.54
19th	24.589	1.216	0.565	3.99	2.42
20th	25.835	1.158	0.537	3.80	2.30
WKB	2.484	12.040	5.588	39.52	23.91

The angular frequency of each mode is given in the rest frame of the plasma (ω) in normalized units. Given a time unit of 4.76 minutes, the time period of the oscillation in the plasma rest frame can be found (τ_p). The period of the mode can be identified with an azimuthal interval in Io's rest frame ($\Delta\phi_I$). To a stationary observer, the mode appears to have a time period of τ_o. This can also be expressed in terms of an interval in the observers Central Meridian Longitude (CML_o).

harmonics and above. The first five velocity and magnetic field eigenmodes calculated from equations (1) and (2) are displayed in Figures 2*a* and 2*b*. Figures 2*c* and 2*d* show the same information but for a much higher frequency, the fourtieth mode. The modes have been normalized according to equation (3) and are orthogonal to better than 0.5%.

The poloidal disturbance has been sketched in previous studies [*Wright and Southwood*, 1987, Figure 11]. According to their calculations a field line grazing Io would have a wave extending along 0.4 R_J of its length (assuming the speed of corotation relative to Io is 57 $km\ s^{-1}$). However, field lines passing through Io would be perturbed over a longer length, as would field lines that do not pass so close to Io as the grazing ones. (Note that the latter lines would also experience a smaller amplitude perturbation.) For these reasons we shall choose 0.8 R_J to represent a typical length along Io's field lines where there is a significant perturbation. This corresponds to a latitude interval of 8°. The poloidal field perturbation is basically bipolar, so we shall model it as two Gaussian distributions of half-width 2° whose centers are offset by 4°. Since there is a north and south bound wave launched, it is possible to simplify the synthesis integrals (6) by considering what happens to the wave behind Io if we reverse time. Both waves will propagate toward the satellite, and (in the absence of Io) will superpose on one another. Due to the symmetry of the north and south bound waves, this superposition is particularly simple; for example, the field perturbations may add together constructivley, and the velocity perturbations could exactly cancel. This requires that $\partial b/\partial t = 0$, and so $J_j = 0$ and all the phases are zero. The coefficients (now given by I_j) may be calculated by the integral in equation (6).

The first synthesis is performed for a disturbance centred on the equator, as may be expected if Io were at the equator. Figures 3*a* and 3*b* show the evolution of the magnetic field perturbation for time intervals 0-5 and 0-10 respectively. (Corresponding azimuths downstream from Io are 0°-11° and 0°-22°.) This synthesis used the first 20 odd field eigenmodes. If Io were not in the equatorial plane, then an asymmetric wave pattern will be produced. This is modeled by moving the bipolar Gassian initial condition by 4° so that the disturbance is confined to one half of the field line only. This initial condition was synthesized from the first 20 odd and even modes, and the evolution is displayed in Figures 4*a* and 4*b*. In both Figures 3 and 4 the bipolar Gaussian wave packet can be seen clearly at $t = 0$. As time increases, the disturbance separates into two waves propagating toward the poles. There is obviously some oscillatory behaviour present. For example, consider the ends of the field lines where there is a large magnetic field perturbation. The large current densities associated with this field will also have an osillatory nature. In Figure 3*a* we can

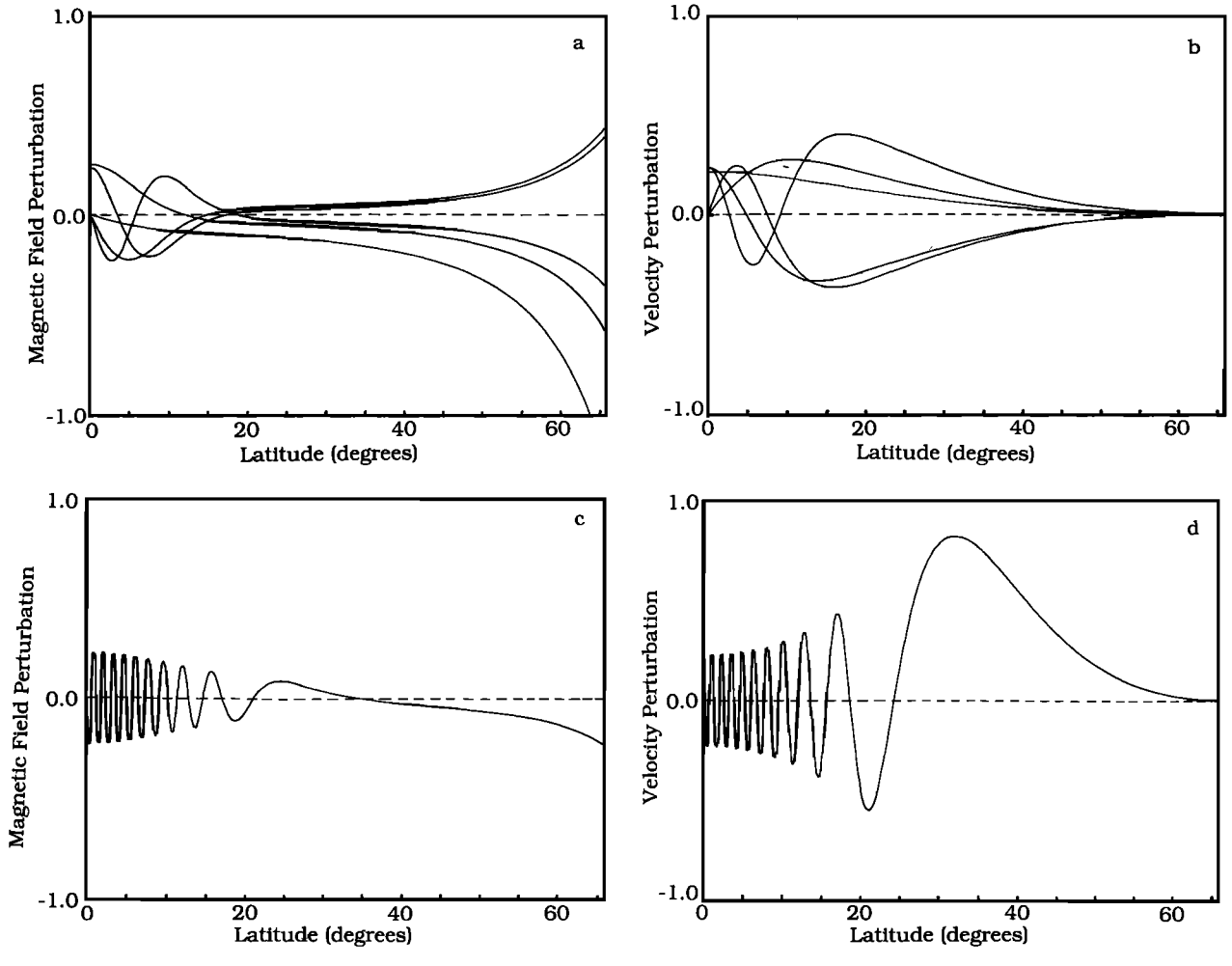

Fig. 2. The poloidal eigenmodes. The magnetic field and velocity perturbations for the first five modes (*a*,*b*), and for the fourtieth mode (*c*,*d*).

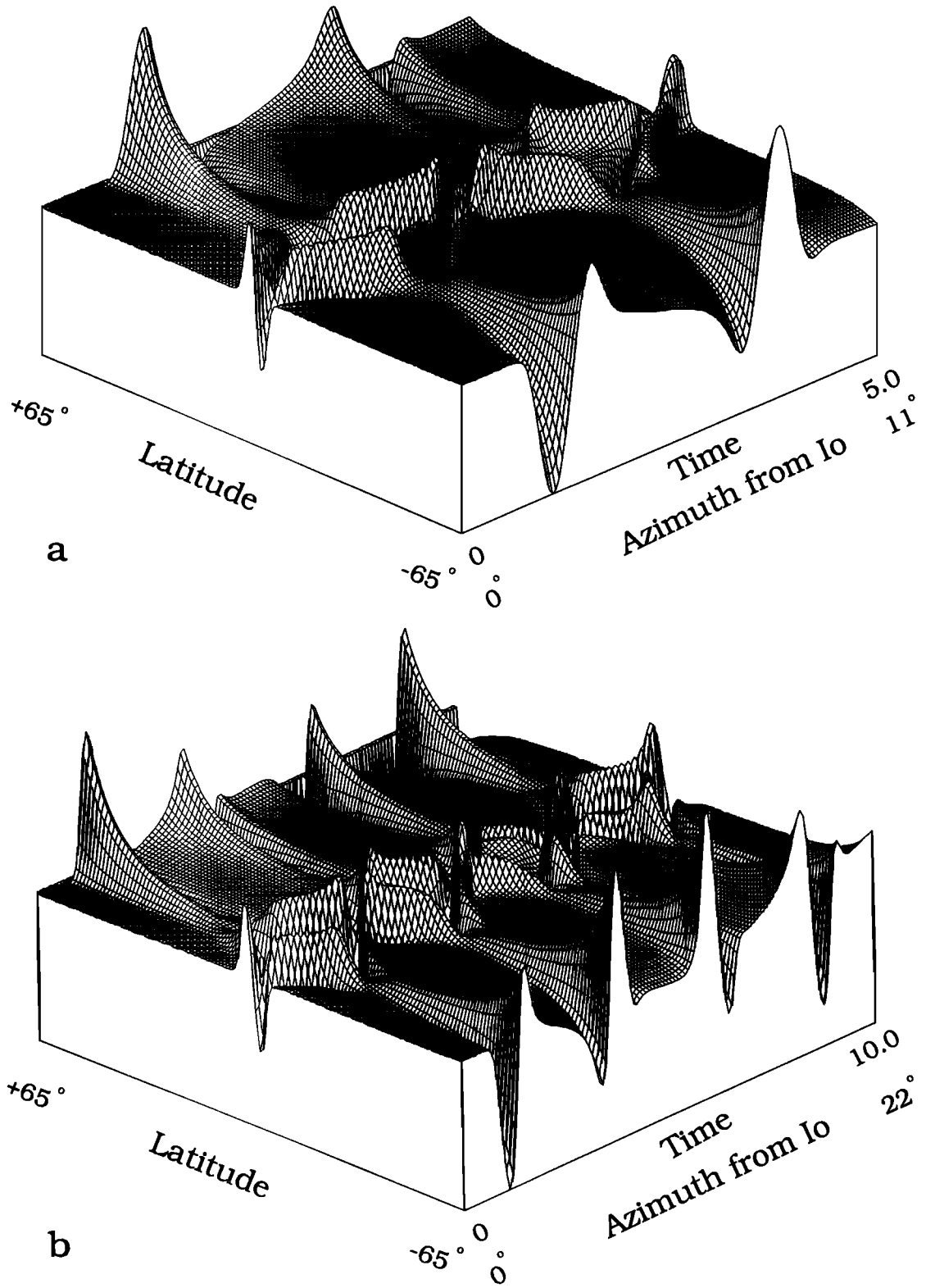

Fig. 3. The evolution of a poloidal perturbation that is symmetrical about the equator. (*a*) Short-term evolution. (*b*) Long-term evolution.

see a strong rise and fall with a period of approximately 2.5. This is not the case for the asymmetric synthesis in Figure 4*a*, where the peaks appear to have a bimodal spacing reminiscent of that suggested by *Gurnett and Goertz* [1981]. The longer-term plots (Figures 3*b* and 4*b*) show this effect quite clearly. These plots also exhibit a long-term modulation as the height of the peaks gradually rises and falls. There is approximately one half of such a cycle in these figures.

In order to study the periods present in Figures 3 and 4 more quantitatively we shall show the intensity spectrum of

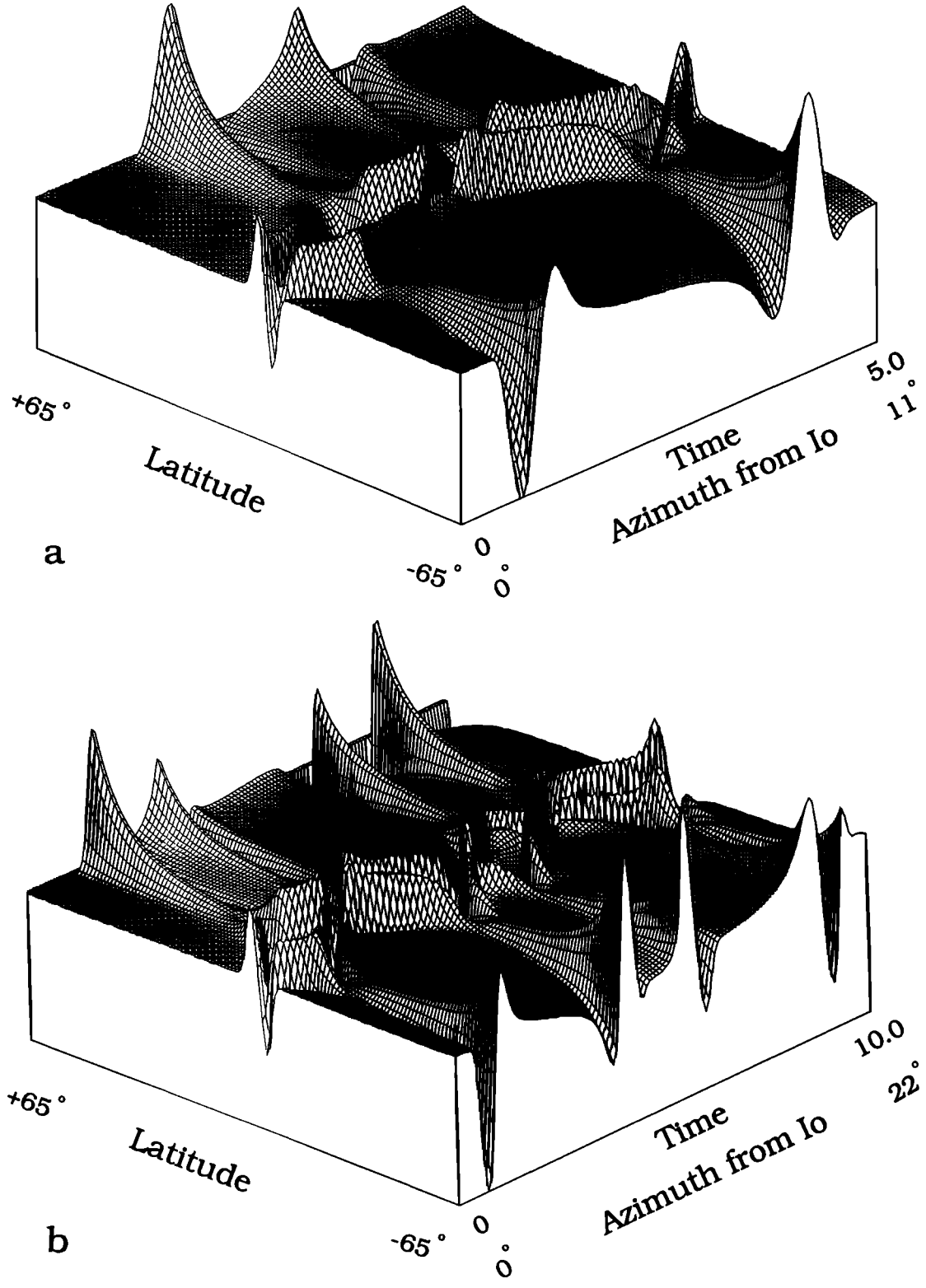

Fig. 4. The same as Figure 3, but for an asymmetrical perturbation.

the field perturbation observed at certain latitudes. These were calculated using a fast Fourier transform over a time interval of 40. (Similar information could also be deduced from the shape of the eigenmodes and the coefficients C_{mj}.) It is interesting to see how the spectra vary with latitude, because the frequency of a DAM emissions is thought be identified with a specific latitude. Figure 5*a* is the spectrum for the symmetric synthesis at a low latitude (8°). This spectrum is very similar to the one for the symmetric synthesis at high latitude (57°) shown in Figure 5*b*. The main difference if that the low frequency modulation is absent in the latter spectrum. The final spectrum (Figure 5*c*) is

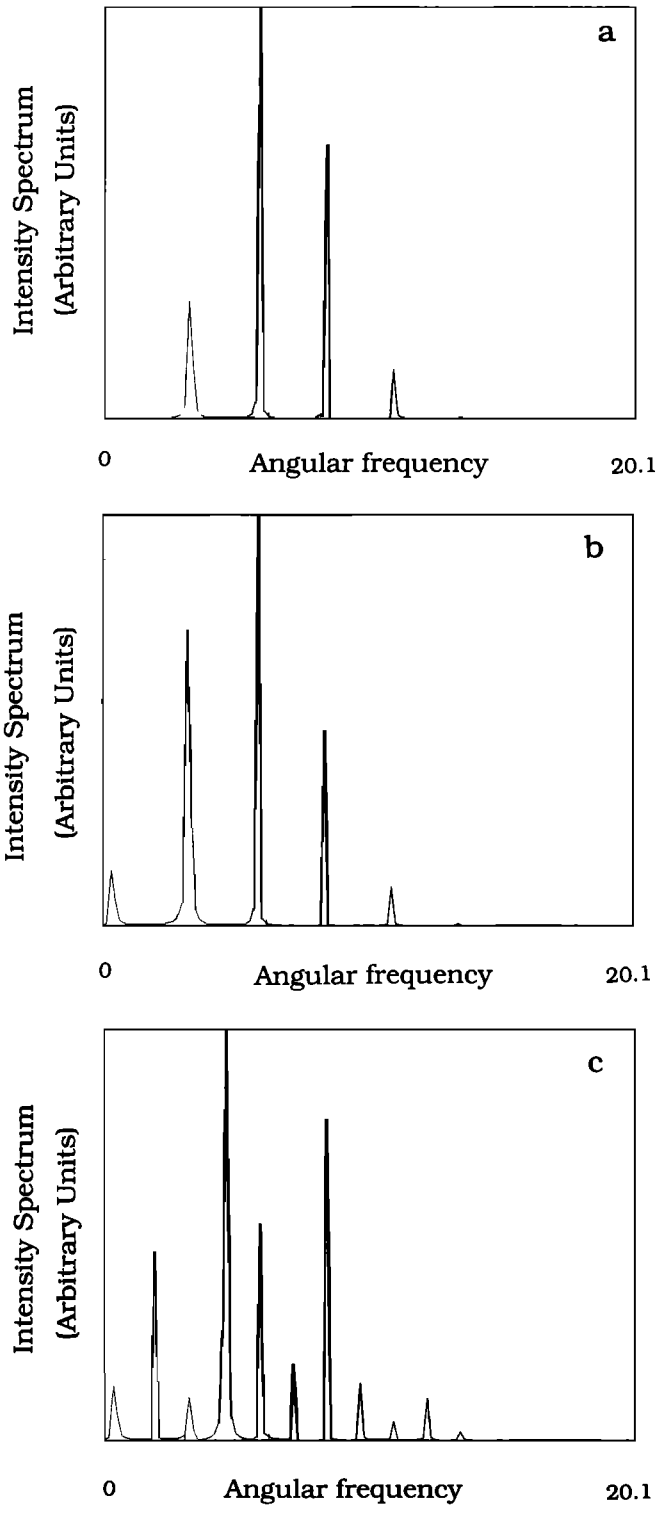

Fig. 5. The intensity spectrum of the magnetic field perturbation. (*a*) Symmetric perturbation measured at 8° latitude. (*b*) Symmetric perturbation measured at 57°. (*c*) Asymmetric perturbation measured at 57°.

also taken at high latitude but is for the asymmetric synthesis. There are many more important frequencies in this spectrum. The low-latitude spectrum for the asymmetric synthesis is similar to the high-latitude one, but the low frequency modulation is absent. Each of the peaks in Figure 5 is assosciated with an eigenmode. In Figure 5*a* the peaks correspond to the 2nd, 4th, 6th, and 8th. This is the same as the spectrum in Figure 5*b* except for the inclusion of the low frequency modulation provided by the fundamental. Figure 5*c* has peaks corresponding to all of the eigenmodes from the fundamental up to the 10th. The dominant frquencies, and the associated intervals are discussed in the next section.

4. Dominant Frequencies and Periods

Before we can compare our periods with those found in data we need to express them in a suitable fashion. For example, data are often expressed in terms of UT (spacecraft event time), or the observer's Jovian longitude (also s/c CML), and most recently in terms of the azimuth or phase downstream from Io. Consider an eigenmode oscillating in the plasma rest frame with eigenfrequency ω. Since the plasma corotates past Io at $\omega_c = 0.4641°\ min^{-1}$ the mode produces an azimuthal periodicity (in Io's rest frame) of $2\pi\omega_c/\omega$. The pattern is fixed in Io's rest frame and so will rotate about Jupiter with Io's orbital angular velocity ($\omega_I = 0.1414°\ min^{-1}$), which gives rise to an observed time period for a fixed observer of $2\pi\omega_c/(\omega_I\omega)$. This time period would be the UT period observed by a spacecraft. Since Jupiter rotates at a rate $\omega_J = 0.605°\ min^{-1}$ the associated Jovian longitude interval of the observer would be $2\pi\omega_c\omega_J/(\omega_I\omega)$. All of the periods and intervals are given as a function of the eigenfrequency in the plasma rest frame (Table 1). Before we compare these periods with observed ones, we shall discuss some of the features of the spectra. For example, why is the low-frequency modulation produced by the fundamental negligible at low latitudes but not at high latitudes? This is a result of the shape of the fundamental mode (see Figure 2). The size of the fundamental mode at 8° is very small; however, it is also very large at high latitudes (at 57° it is about 7 times larger; see Figure 2). This is probably why the effect of the fundamental mode is negligible at low latitudes.

Another interesting feature of the spectra is the fact that there is a well defined band-width, and maximum intensities occur for the 4th to 6th harmonics typically. This is evidently related to our choice of initial conditions. We used a disturbance that spans 8° of latitude near the equator. The "wavelength" of this corresponds to 0.8 R_J. The equatorial Alfvén speed was chosen to be $V_{Aeq} = 250\ km\ s^{-1}$, so the assosciated frequency is $\omega = 8$. This frequency lies between the eigenfrequencies of the 5th and 6th harmonics, which are indeed near the centre of the intensity spectra. Our choice of initial disturbance was taken to represent a typical field line in the Alfvén wings. We know that some field lines (like the ones grazing Io) will have an initial perturbation of half the length of those used in the simulation. For example, the grazing field lines will have an assosciated frequency of 16, and we would expect the intensity spectrum for this initial condition to be centered on 12th or 13th harmonics. This would provide much more small-scale structure in the wake than those shown in Figures 3 and 4. These properties should not be affected by uniform variations in the plasma density. Consider the situation when the plasma density is increased everywhere by a given factor. The Alfvén speed will decrease and so will the length of the perturbation along the field line (both by the same amount). As a result, the real period associated with the disturbance is unaltered (the

normalized period will increase). The intensity spectrum for the increased density case will have its peaks shifted to higher modes whose real eigenfrequencies are similar to the real eigenfrequencies of the 4th to 6th modes in the unaltered density case. As a result, the periods and intervals expected are unaffected by a uniform change in density. An interesting limit is when the plasma density increases to such an extent that the WKB limit is valid everywhere. In this situation the synthesis becomes a Fourier series for the WKB solution viewed at a given latitude. (These circumstances will never be realized in practice.)

The results we have presented here are dependent upon our model field and density distribution. The field in Io's L shell can be approximated to a dipole field to within 10%. The density distribution is much more uncertain, especially at mid-latitudes (10°-30°). The actual density distribution may be different from the one assumed here. It is known that the transmission of waves through the torus is sensitive to the scale length of the Alfvén speed variation [*Wright and Schwartz*, 1989]. In this paper we have been looking for periodic structure in the waves launched from Io, and should consider how our conclusions would be modified by a change in density profile. It turns out that the spectra in Figure 5 and the intervals in Table 1 are relativley insensitive to the density at mid-latitudes for the following reasons: The round-trip travel time for an Alfvén wave is basically governed by the time to traverse the center of the torus, since this is where the propagation speed is slowest. Hence uncertainties in the density at mid-latitudes will not affect the round-trip travel time very much, especially as they modulate the group velocity via a square root. Thus we expect our estimate of an Alfvén wave round-trip travel time of 24 *min* to be reliable. Now let us consider the effect of a change in mid-latitude densities upon the eigenfrequencies and intensity spectra (Figure 5). We have already pointed out that the WKB estimates of the eigenfrequencies ($\omega_j = \frac{1}{2}(j+1)\omega_B$) are very close to the eigenfrequencies determined numerically for the third harmonic and above. Since ω_B is based upon the Alfvén travel time (which we do not expect to change much), it follows that the eigenfrequencies ω_j ($j > 2$) will not change by a significant amount either. The first three eigenfrequencies (ω_0, ω_1, and ω_2) may, or may not, be modified from their original values. However, given that they satisfy $0 < \omega_0 < \omega_1 < \omega_2 < \omega_3$, and ω_3 is approximately unchanged, it seems likely that there will only be a small margin of deviation. Thus the eigenfrequencies in the intensity spectra will be qualitatively the same as in Figure 5 and quantitatively only slightly different. The height of the peaks may change a little, but again we do not anticipate any major differences since the arguments given in the preceding paragraph can still be used to predict the location of the maximum in the spectrum. The general character of Figure 5 will certainly be preserved by changes of the density distribution at mid-latitudes.

5. DAM OBSERVATIONS

Now we shall turn our attention to periods found in decametric data. It should be borne in mind that intervals quoted in Table 1 are based upon a time unit of 4.76 *min* providing a round trip time of 24.1 *min*. These can be changed as better estimates become availiable and the intervals scaled appropriately. Since each interval corresponds to an upward and a downward current, it is possible that they may modulate emissions on a scale of half this interval. We shall begin with the larger scale features. The fundamental mode is expected to produce a modulation on a scale of 160° (possibly 80°) in Jovian longitude, or CML. It is also expected that this modulation be most evident at high latitudes, i.e., high DAM frequencies. Such a long interval may be identified with the length of a DAM storm. The data presented by *Leblanc and Genova* [1981, Figure 1*a*] and *Leblanc* [1981, Figures 9*a* and 9*b*] show storms that extend over either 70° or 180° of CML. It is difficult to estimate the extent of the storm displayed in Figure 1, but a duration of about 70° CML seems reasonable. It is interesting to note that without exception, all of these storms show a much greater modulation of the higher-frequency emissions than the lower-frequency ones, as we expect from an effect produced by the fundamental.

In addition to the large-scale associated with a storm, there is medium-scale structure like the bunching of arcs in Figure 1 (this is particularly clear in the second panel). The bunching of arcs is often seen as an enhancement of the DAM emissions during a storm in low-resolution data. The period is about 16° (in s/c CML) and could be due to stucture associated with the second harmonic, or perhaps half the period of the first harmonic. On a smaller scale there is the separation of individual arcs. In Figure 1 a typical arc separation is approximately 3°-4° (s/c CML) which is close to the value found by *Staelin et al.* [1988] of 4-7 *min* (s/c UT), equivalent to 2.5°-4° s/c CML. Staelin et al. point out that this is about 2.7 times less than the WKB periodicity. These intervals could be produced by the 11th to 18th harmonics, which should be well represented in the synthesis for field lines grazing Io. Alternatively, if the 5th to 9th harmonics may produce DAM structure on half of their ocsillation period, this could also account for the arc separation. Improved emission models are required before we can decide which is the more likely explanation.

6. CONCLUDING REMARKS

We have modeled the long-term evolution of Io's Alfvén waves by a normal mode analysis. We do not find WKB behavior (except in the immediate vicinity of the satellite). However, we do find several important periodicities in the wake that span large-, medium- and small-scale structure ($> 60°$, 60°-6°, $< 6°$ s/c CML, respectively). As suggested by *Wright* [1987*b*], the higher harmonics can produce finer structure in the DAM spectra, which may be able to account for the arc separation and the bunching of arcs within a storm. The length of a storm may well be associated with the fundamental mode. This is also supported by the fact that the greatest modulation is seen at high frequencies. Future work will consider the short comings of the decoupled transverse field modes. In particular, whether a wave localized across the background magnetic field need evolve a compressional component. The effect of a parallel field perturbation on our results is not clear. However, it is likely that such coupling may simply act as a damping mechanism if b_γ is much less than b_α or b_β.

APPENDIX

Throughout this appendix we shall make use of magnetic field-aligned coordinates (α, β, γ). The coordinates (α, β)

are constant on a field line, and $\hat{\gamma}$ is parallel to the background magnetic field, $\mathbf{B} = (0, 0, B)$. The geometry of the field is contained in a set of geometrical scale factors $h_i = \hat{\mathbf{i}}/\nabla i$, where $i = \alpha, \beta, \gamma$, [e.g., *Davis and Snider*, 1979]. Using standard results we may write

$$\nabla.\mathbf{B} = 0 = \frac{\partial}{\partial\gamma}(Bh_\alpha h_\beta) \tag{A1}$$

This has the general solution $Bh_\alpha h_\beta = f(\alpha, \beta)$, which states that the product of magnetic field strength and tube cross section is constant for a given flux tube. The magnetic field may be obtained by inverting this relationship:

$$\mathbf{B} = \hat{\gamma} \cdot \frac{f(\alpha,\beta)}{h_\alpha h_\beta} = f(\alpha,\beta) \cdot \nabla\alpha_\wedge\nabla\beta \tag{A2}$$

Clearly, if α and β are equal to matched Euler potentials (α_e, β_e), then f is equal to unity, or if (α, β) are a linear sum of (α_e, β_e), then f is a constant. More generally, f is found from the Jacobian of the mapping between α and β and the Euler potentials,

$$f(\alpha,\beta) = J\left(\frac{(\alpha_e,\beta_e)}{(\alpha,\beta)}\right) = \frac{\partial\alpha_e}{\partial\alpha}\cdot\frac{\partial\beta_e}{\partial\beta} - \frac{\partial\alpha_e}{\partial\beta}\cdot\frac{\partial\beta_e}{\partial\alpha} \tag{A3}$$

The background current can be found by using Ampere's law,

$$\nabla_\wedge\mathbf{B} = \frac{1}{h_\alpha h_\beta h_\gamma}\left(\hat{\alpha}h_\alpha\frac{\partial(Bh_\gamma)}{\partial\beta} + \hat{\beta}h_\beta\frac{\partial(Bh_\gamma)}{\partial\alpha} + 0\hat{\gamma}\right) \tag{A4}$$

Note that there can not be any background field-aligned current in this coordinate system if it is to be single valued (see also *Walker* [1987]). If the background field is a potential field, equation (A4) tells us that Bh_γ is a function of γ alone, say $g(\gamma)$.

$$h_\gamma = \frac{g(\gamma)}{B} = g(\gamma)\cdot\frac{f(\alpha,\beta)}{h_\alpha h_\beta} \tag{A5}$$

Evidently $1/B$ determines the form of the surfaces $\gamma =$ const, while $g(\gamma)$ specifies the value of γ on each surface. Suppose we are interested in the motion of a specific field line (α_o, β_o). A suitable choice for g would be $g = B(\alpha_o, \beta_o, \gamma)$, in which case $h_\gamma(\alpha_o, \beta_o, \gamma) = 1$, and γ will be equal to the distance along the field line $(\alpha_o, \beta_o, \gamma)$. (On other field lines, γ will only be proportional to the path length along that line.)

In this coordinate system the perturbed cold plasma momentum equation may be written [e.g., *Wright*, 1987*b*]

$$\frac{\mu_o\rho}{B}\cdot\frac{\partial\mathbf{u}}{\partial t} = \frac{\hat{\alpha}}{h_\alpha h_\gamma}\cdot\left(\frac{\partial(b_\alpha h_\alpha)}{\partial\gamma} - \frac{\partial(b_\gamma h_\gamma)}{\partial\alpha}\right) + \frac{\hat{\beta}}{h_\beta h_\gamma}\cdot\left(\frac{\partial(b_\beta h_\beta)}{\partial\gamma} - \frac{\partial(b_\gamma h_\gamma)}{\partial\beta}\right) + \hat{\gamma}0 \tag{A6}$$

while the perturbed induction equation can be written as follows:

$$\frac{\partial\mathbf{b}}{\partial t} = \frac{\hat{\alpha}}{h_\beta h_\gamma}\cdot\frac{\partial}{\partial\gamma}(h_\beta u_\alpha B) + \frac{\hat{\beta}}{h_\alpha h_\gamma}\cdot\frac{\partial}{\partial\gamma}(h_\alpha u_\beta B) - \frac{\hat{\gamma}}{h_\alpha h_\beta}\cdot\left(\frac{\partial}{\partial\alpha}(h_\beta u_\alpha B) + \frac{\partial}{\partial\beta}\cdot(h_\alpha u_\beta B)\right) \tag{A7}$$

For a background potential field, the γ component of the induction equation may be written in the equivalent form

$$\frac{\partial b_\gamma}{\partial t} = -h_\gamma\nabla.[\mathrm{u}_\perp B/h_\gamma] = \frac{-1}{B}\nabla\cdot[\mathrm{u}_\perp B^2] \tag{A8}$$

Note that not all of the h_γ factors are included in the appendix of *Wright* [1987*b*]; however, this does affect the equations that he solved.

Acknowledgments. The authors would like to thank D.A. Gurnett for kindly supplying Figure 1. This work was performed while A.N.W. was a UK SERC Fellow and Research Assistant.

The editor thanks K.K. Khurana and another referee for their assistance in evaluating this paper.

REFERENCES

Acuña, M. H., F. M. Neubauer, and N. F. Ness, Standing Alfvén wave current system at Io: Voyager 1 observations, *J. Geophys. Res., 86,* 8513, 1981.

Acuña, M. H., K. W. Behannon, and J. E. P. Connery, Jupiter's Magnetic Field and Magnetosphere, in *Physics of the Jovian Magnetosphere,* edited by A. J. Dessler, Cambridge University Press, New York, 1983.

Bagenal, F., Alfvén wave propagation in the Io plasma torus, *J. Geophys. Res., 88,* 3013, 1983.

Bagenal, F., and Y. Leblanc, Io's Alfvén wave pattern and the Jovian decametric arcs, *Astron. Astrophys., 197,* 311, 1988.

Barnett, A. S., In situ measurements of the plasma bulk velocity near the Io flux tube, *J. Geophys. Res., 91,* 3011, 1986.

Barnett, A., and S. Olbert, Radiation of plasma waves by a conducting body moving through a magnetized plasma, *J. Geophys. Res., 91,* 10,117, 1986.

Belcher, J. W., C. K. Goertz, J. D. Sullivan, and M. H. Acuña, Plasma observations of the Alfvén wave generated by Io, *J. Geophys. Res., 86,* 8508, 1981.

Bigg, E. K., Influence of the satellite Io on Jupiter's decametric emission, *Nature, 203,* 1008, 1964.

Bridge, H. S., et al., Plasma observations near Jupiter: Initial results from Voyager 1, *Science, 204,* 987, 1979.

Broadfoot, A. L., et al., Extreme ultraviolet observations from Voyager 1 encounter with Jupiter, *Science, 204,* 979, 1979.

Brown, R. A., Optical line emission from Io, in *Exploration of the Planetary System,* edited by A. Woszczyk and C. Iwaniszewska, D. Riedel, Hingham, Mass., 1974.

Carnaham, B., H. A. Luther, and J. O. Wilkes, *Applied numerical methods,* John Wiley, New York, 1969.

Davis, H. F., and A. D. Snider, *Introduction to Vector Analysis,* Allyn and Bacon, London, 1979.

Drell, S. D., H. M. Foley, and M. A. Ruderman, Drag and propulsion of large satellites in the ionosphere, *J. Geophys. Res., 70,* 3131, 1965.

Dungey, J. W., Hydromagnetic waves, in *Physics of Geomagnetic Phenomena,* vol. 2, edited by S. Matsushita and W. H. Campbell, pp. 913–934, Academic, San Diego, Calif., 1967.

Goertz, C. K., Io's interaction with the plasma torus, *J. Geophys. Res., 85,* 2949, 1980.

Goertz, C. K., and P. A. Deift, Io's interaction with the magnetosphere, *Planet. Space Sci., 21,* 1399, 1973.

Goldreich, P., and D. Lynden-Bell, Io, a Jovian unipolar inductor, *Astrophys. J., 156,* 59, 1969.

Goldstein, B. E., and W.-H. Ip, Magnetic drifts at Io: Depletion of 10-MeV electrons at Voyager 1 encounter due to a forbidden zone, *J. Geophys. Res., 88,* 6137, 1983.

Goldstein, M. L., and C. K. Goertz, Theories of radio emissions and plasma waves, in *Physics of the Jovian Magnetosphere,* edited by A. J. Dessler, Cambridge University Press, New York, 1983.

Gurnett, D. A., and C. K. Goertz, Multiple Alfvén wave reflections excited by Io: Origin of the Jovian decametric arcs, *J. Geophys. Res., 86,* 717, 1981.

Herbert, F., "Alfvén wing" models of the induced current system at Io: A probe of the ionosphere of Io, *J. Geophys. Res., 90,* 8241, 1985.

Lanzerotti, L. J., C. G. Maclennan, T. P. Armstrong, S. M. Krimigis, R. P. Lepping, and N. F. Ness, Ion and electron angular

distributions in the Io torus region of the Jovian magnetosphere, *J. Geophys. Res., 86,* 8491, 1981.

Leblanc, Y., On the arc structure of the DAM Jupiter emissions, *J. Geophys. Res., 86,* 8546, 1981.

Leblanc, Y., and F. Genova, The Jovian *S* burst sources, *J. Geophys. Res., 86,* 8564, 1981.

Linker, J. A., M. G. Kivelson, and R. J. Walker, A MHD simulation of plasma flow past Io: Alfvén and slow mode perturbations, *Geophys. Res. Lett., 15,* 1311, 1988.

Neubauer, F. M., Nonlinear standing Alfvén wave current system at Io: Theory, *J. Geophys. Res., 85,* 1171, 1980.

Radoski, H. R., Highly asymmetrical MHD resonances: The guided poloidal mode, *J. Geophys. Res., 72,* 4026, 1967.

Schulz, M., and A. Eviatar, Charged particle absorption by Io, *Astrophys. J. Lett., 211,* L149, 1977.

Singer, H. J., D. J. Southwood, R. J. Walker, and M. G. Kivelson, Alfvén wave resonances in a realistic magnetospheric magnetic field geometry, *J. Geophys. Res., 86,* 4589, 1981.

Smith, P. R., and A. N. Wright, Multiscale periodic structure in the Io wake, *Nature, 339* 452, 1989.

Southwood, D. J., M. G. Kivelson, R. J. Walker, and J. A. Slavin, Io and its plasma environment, *J. Geophys. Res., 85,* 5959, 1980.

Staelin, D. H., P. M. Garnavich, and Y. Leblanc, Jovian decametric arcs and currents, *J. Geophys. Res., 93,* 3942, 1988.

Walker, A. D. M., Theory of magnetospheric standing hydromagnetic waves with large azimuthal wave number, 1. Coupled magnetosonic and Alfvén modes, *J. Geophys. Res., 92,* 10,039, 1987.

Walker, R. J., and M. G. Kivelson, Multiply reflected standing Alfvén waves in the Io torus: Pioneer 10 observations, *Geophys. Res. Lett., 8,* 1281, 1981.

Warwick, J. W., et al., Voyager 1 planetary radio astronomy observations near Jupiter,*Science, 204,* 995, 1979*a*.

Warwick, J. W., et al., Planetary radio astronomy observations from Voyager 2 near Jupiter,*Science, 206,* 991, 1979*b*.

Wolf-Gladrow, D. A., F. M. Neubauer, and M. Lussem, Io's interaction with the plasma torus: A self-consistent model, *J. Geophys. Res., 92,* 9949, 1987.

Wright, A. N., Energetic particle absorption at Io, *J. Geophys. Res., 92,* 3155, 1987*a*.

Wright, A. N., The interaction of Io's Alfvén waves with the Jovian magnetosphere, *J. Geophys. Res., 92,* 9963, 1987*b*.

Wright, A. N., and S. J. Schwartz, The transmission of Io's Alfvén waves through the Io plasma torus, *J. Geophys. Res., 94,* 3749, 1989.

Wright, A. N., and D. J. Southwood, Stationary Alfvénic Structures, *J. Geophys. Res., 92,* 1167, 1987.

P. R. Smith, Electronic and Electrical Engineering Department, University of Loughborough, Leicestershire LE11 3TU, England.

A. N. Wright, Astronomy Unit, School of Mathematical Sciences, Queen Mary and Westfield College, London E1 4NS, England.

(Received May 15, 1989;
revised July 24, 1989;
accepted August 21, 1989.)